

## Temperature dependence of current transport in Al/Al<sub>2</sub>O<sub>3</sub> nanocomposite thin films

Y. Liu,<sup>1,a)</sup> T. P. Chen,<sup>2,b)</sup> L. Ding,<sup>2</sup> M. Yang,<sup>2</sup> Z. Liu,<sup>2</sup> J. I. Wong,<sup>2</sup> and S. Fung<sup>3</sup>

<sup>1</sup>State Key Laboratory of Electronic Thin Films and Integrated Devices, University of Electronic Science and Technology of China, Chengdu, Sichuan, 610054, People's Republic of China

<sup>2</sup>School of Electrical and Electronic Engineering Nanyang Technological University, Singapore 639798

<sup>3</sup>Department of Physics, The University of Hong Kong, Pokfulam, Hong Kong

(Received 7 July 2011; accepted 26 October 2011; published online 15 November 2011)

In this work, Al/Al<sub>2</sub>O<sub>3</sub> nanocomposite thin film is deposited on Si substrate by radio frequency sputtering to form a metal-insulator-semiconductor structure. It is found that the current conduction at low fields is greatly enhanced with temperature. The current increase can be attributed to the decrease in the tunneling resistance and/or the formation of some tunneling paths due to the release of some measurement-induced charges trapped in the thin film as a result of increase in the temperature. The current conduction evolves with a trend toward a three-dimensional transport as the temperature increases. © 2011 American Institute of Physics. [doi:10.1063/1.3663313]

### INTRODUCTION

Intensive research have been carried out on Al<sub>2</sub>O<sub>3</sub> due to its excellent electrical properties such as low leakage current, high dielectric constant (~9), and high breakdown voltage (~9 MV/cm). The material is considered as a promising candidate for the gate dielectric of field-effect transistors.<sup>1-3</sup> Various techniques such as radio-frequency magnetron sputtering,<sup>4</sup> atomic-layer-deposition (ALD),<sup>5</sup> and plasma-enhanced atomic-layer deposition (PEALD)<sup>6</sup> have been used to prepare the Al<sub>2</sub>O<sub>3</sub> films. Recently, it was reported that Al-rich Al<sub>2</sub>O<sub>3</sub> thin film can be used to realize resistive memory device<sup>7</sup> and floating gate non-volatile memory device.<sup>8</sup> As those memory devices may work at elevated temperatures, the temperature dependence of current conduction in the Al-rich Al<sub>2</sub>O<sub>3</sub> layer of the metal-insulator-metal structure for resistive memory device or in the gate dielectric for the floating gate memory device is important. On the other hand, some studies on the current conduction mechanism of semiconductor nanocrystals embedded in oxide film have been reported.<sup>9-11</sup> Mechanisms including Fowler-Nordheim (FN) tunneling, nanocrystal-assisted tunneling, Frenkel-Poole emission and nanocrystal-assisted FN tunneling have been proposed.<sup>9</sup> However, the mechanism of conduction in metal/dielectric nanocomposite films has seldom been discussed. In this work, Al<sub>2</sub>O<sub>3</sub> film is deposited on Si substrate by radio frequency (RF) sputtering of Al target in O<sub>2</sub> ambient to form a metal-insulator-semiconductor (MIS) structure. Transmission Electron Microscopy (TEM) image shows that Al/Al<sub>2</sub>O<sub>3</sub> nanocomposite thin films are formed. The influence of temperature on current transport at low fields in Al/Al<sub>2</sub>O<sub>3</sub> nanocomposite films has been studied. It is found that the current conduction is greatly enhanced with temperature. The current-voltage (*I-V*) characteristics at low fields follow a power law. As the temperature increases, the system

evolves with a trend toward a three-dimensional (3D) transport. The phenomena can be explained by a model of charge transport in the Al nanocrystal arrays.

One hundred nm thick Al-rich Al<sub>2</sub>O<sub>3</sub> films were deposited on p-type, (100)-oriented Si wafers via radio frequency magnetron sputtering. The deposition was carried out with RF sputtering of Al target (purity > 99.999%) in O<sub>2</sub>/Ar ambient at a power of 310 W. The Ar to O<sub>2</sub> ratio is set to 60:1. The films were annealed with rapid thermal process at 500 °C for 2 min. A 200 nm aluminum layer was then deposited on the top of the thin films to form gate electrodes. The backside electrode was formed with a 500 nm aluminum layer after removing initial oxide. The high resolution transmission electron microscopy (HRTEM) image shows the existence of Al nanocrystals (nc-Al) (or nanoparticles) in the Al oxide layer, as illustrated in Fig. 1. The *I-V* measurements were carried out with a Keithley 4200 semiconductor characterization system, and capacitance-voltage (*C-V*) measurements were carried out with a HP4284 A LCR meter at the frequency of 1 MHz.

Figure 2 shows the *I-V* characteristics measured at low fields at 25 °C, 75 °C, and 100 °C, respectively. As can be seen in the figure, the current conduction is greatly enhanced by increasing the temperature. The conduction enhancement can be explained as following. Electron tunneling can take place between adjacent uncharged Al nanocrystals, and many such nanocrystals form tunneling paths connecting the Si substrate to the metal gate.<sup>9,12,13</sup> As reported in our previous works<sup>13,14</sup> electrons can be trapped in the nanocrystals when they transport along the tunneling paths during a current measurement, causing a reduction in the current conduction due to the Coulomb interactions, whereas the release of the trapped charges leads to an increase in the current conduction. In the Al/Al<sub>2</sub>O<sub>3</sub> nanocomposite thin film, even in the initial state, there may be some electrons trapped in nanocrystals during the electrical measurement. The trapped charges can be released when the temperature is increased, making more nanocrystals neutral (uncharged). With the existence of more tunneling paths formed by the uncharged

<sup>a)</sup>Author to whom correspondence should be addressed. Electronic mail: yliu2008@e.ntu.edu.sg.

<sup>b)</sup>Electronic mail: echentp@ntu.edu.sg.

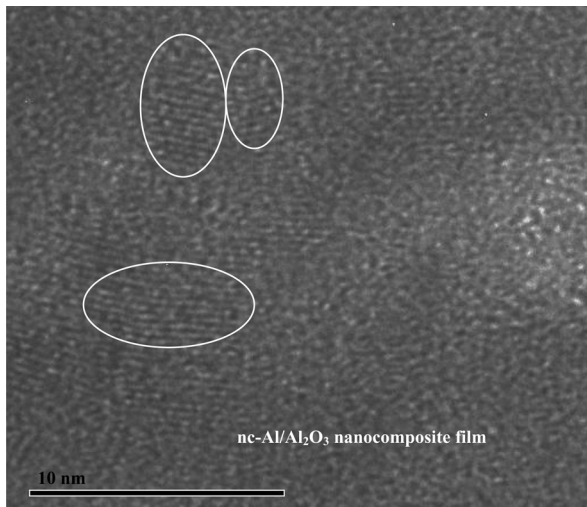


FIG. 1. TEM image of the Al/Al<sub>2</sub>O<sub>3</sub> nanocomposite thin film.

nanocrystals, the current conduction of the thin film system is enhanced. The charge release is confirmed by the  $C$ - $V$  measurements, as shown in the inset of Fig. 2. With temperature increasing, the  $C$ - $V$  characteristic is shifted to the negative-voltage side, which indicates electron release from the nanocomposite thin film at a higher temperature. The flatband voltage shift is proportional to the amount of the charges released from the Al/Al<sub>2</sub>O<sub>3</sub> nanocomposite film. The charge release leads to an enhancement in the current conduction as well as a higher dimensional transportation in the oxide thin film, which will be discussed later.

Figure 2 shows that the  $I$ - $V$  characteristics at low fields follow a power law. The power-law behavior could be explained by a model similar to the one of collective charge transport in arrays of normal-metal quantum dots (QDs).<sup>15</sup> The current through an array of metallic quantum dots separated by tunnel barriers is shown to follow the power-law relationship<sup>15,16</sup>

$$I = I_0(V - V_{th})^\zeta, \quad (1)$$

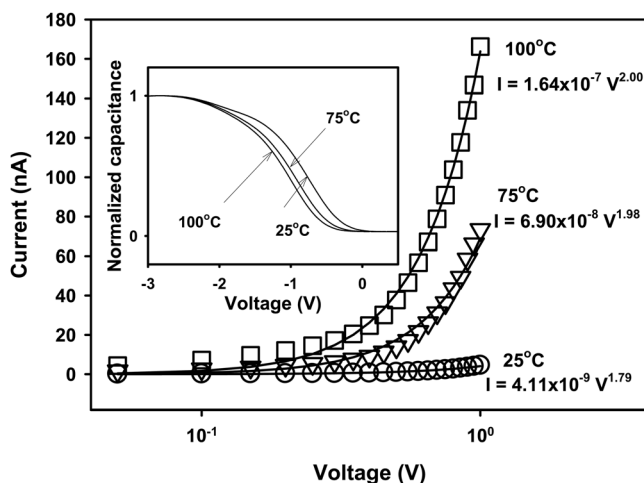


FIG. 2.  $I$ - $V$  characteristics at low fields measured at 25°C, 75°C, and 100°C, respectively. The inset shows the  $C$ - $V$  characteristics at the corresponding temperatures. The solid lines show the fittings based on Eq. (1).  $I_0 = 4.11 \times 10^{-9} \text{ AV}^{-\zeta}$  and  $\zeta = 1.79$  at 25°C;  $I_0 = 6.90 \times 10^{-8} \text{ AV}^{-\zeta}$  and  $\zeta = 1.98$  at 75°C; and  $I_0 = 1.64 \times 10^{-7} \text{ AV}^{-\zeta}$  and  $\zeta = 2.00$  at 100°C.

where  $\zeta$  is the scaling exponent, and  $V_{th}$  is the threshold voltage. The scaling exponent  $\zeta = 1$  and  $5/3$  correspond to the one- and two-dimensional arrays of QDs, respectively.<sup>15,16</sup> Equation (1) can be used to fit our experimental result of the system of Al/Al<sub>2</sub>O<sub>3</sub> nanocomposite film, and the fitting can yield the values of the factors including  $\zeta$ ,  $V_{th}$  and  $I_0$  of Eq. (1). The threshold voltage is found to be approximately zero. Figure 3 shows Arrhenius plot of  $\ln(I_0)$  and  $\zeta$  obtained from the fittings.  $\zeta$  is found to be larger than  $5/3$ . This suggests that the current conduction in the system is a quasi-3D transport. With temperature increasing, some of trapped charges are released from the nanocrystals, leading to formation of some new tunneling paths. With the formation of new tunneling paths, the current conduction of the system will evolve toward a higher dimensional transport, i.e., quasi-3D transport. On the other hand,  $I_0$  is observed to increase with temperature. For the case shown in Fig. 3,  $I_0$  increases greatly from the initial  $I_0 = 4.12 \times 10^{-9} \text{ AV}^{-\zeta}$  at 25°C to  $I_0 = 5.60 \times 10^{-6} \text{ AV}^{-\zeta}$  at 200°C.

As indicated in Fig. 3, the temperature increase leads to an increase in both  $I_0$  and  $\zeta$ . The increase in  $I_0$  is attributed to the decrease of the tunneling resistance and/or the increase in the number of tunneling paths as a result of the charge release at a higher temperature. The activation energy obtained from the Arrhenius plot of  $I_0$  is 0.52 eV, indicating that the barrier for charge releasing is around 0.5 eV. On the other hand,  $\zeta$  increases from 1.79 at 25°C to 2.10 at 200°C, showing an evolution with a trend toward the 3D transport when more charges are released at a higher temperature.

As mentioned above, the increases in both  $\zeta$  and  $I_0$  are due to the release of the charges trapped in the nanocrystals at a higher temperature. To confirm the charge release,  $C$ - $V$  measurement is carried out to determine the flatband voltage shift which is proportional to the amount of the charges released. As shown in the inset of Fig. 2, the  $C$ - $V$  curve shifts toward the negative-voltage side when the temperature increases, showing a negative flatband voltage shift. The negative flatband voltage shift indicates a reduction in the amount of electrons trapped in the nanocomposite film. The electron release is due to the electron escape from nanocrystals at a higher temperature. Note that the  $C$ - $V$  measurement is affected by the charge trapping in the oxide layer and is most sensitive to the charges in the oxide region near the Al<sub>2</sub>O<sub>3</sub>/Si interface.

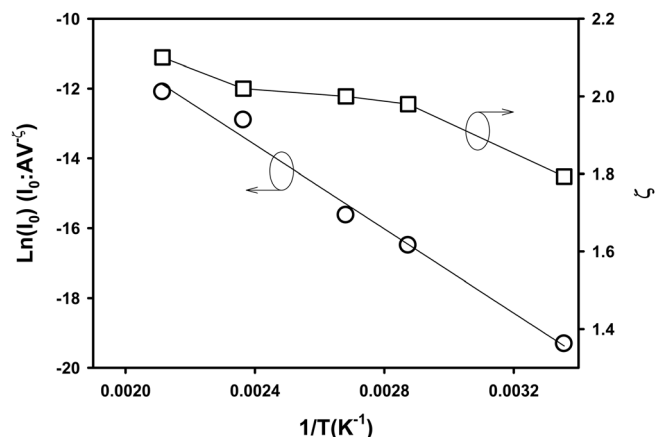


FIG. 3. Arrhenius plots of  $I_0$  and  $\zeta$ .

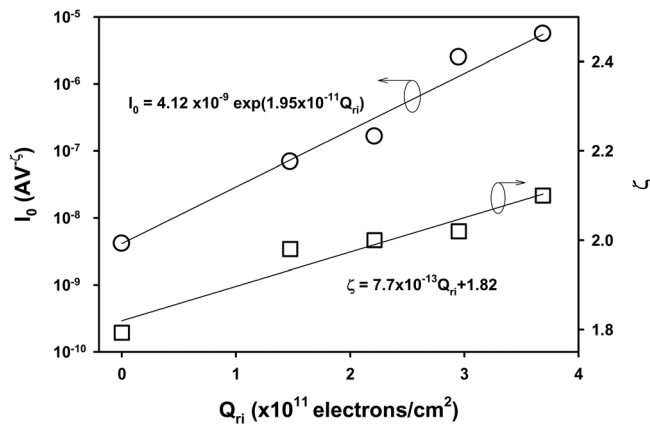


FIG. 4.  $I_0$  and  $\zeta$  as a function of  $Q_{ri}$ . Note that  $Q_{ri}=0$  at room temperature, which is taken as the reference. The change of  $Q_{ri}$  is realized by changing the temperature. The solid lines show the fittings.

Therefore, the electron release from the oxide layer is described with the equivalent areal charge density ( $Q_{ri}$ ) calculated from the flatband voltage shift ( $\Delta V_{FB}$ ), i.e.,  $Q_{ri} = C_{ox}\Delta V_{FB}$  where  $C_{ox}$  is the oxide capacitance per area. Note that the initial flat-band voltage at room temperature ( $25^\circ\text{C}$ ) is taken as the reference for calculating  $\Delta V_{FB}$  and thus  $Q_{ri}$  is zero at room temperature. Assuming the charge uniformly distributes in the oxide film, the total amount of charges released from the film is proportional to  $Q_{ri}$ . Thus, the temperature dependence of  $\Delta V_{FB}$  is translated into the temperature dependence of  $Q_{ri}$ . To study the effect of charge release on the current transport, electron releases with different amounts from the nanocrystals are achieved by raising the temperature to different levels. For a given temperature,  $Q_{ri}$  is obtained from the flatband voltage shift based on the  $C$ - $V$  measurement as discussed above, and  $I_0$  and  $\zeta$  are obtained from the fittings to the  $I$ - $V$  characteristics. In this way, we are able to examine the influence of electron release from nanocrystals on  $I_0$  and  $\zeta$ . Figure 4 shows  $I_0$  and  $\zeta$  as a function of  $Q_{ri}$ .

Electron tunneling can take place between adjacent uncharged nanocrystals, and many such nanocrystals form conduction paths connecting the Si substrate to the metal gate.<sup>12,13</sup> As nanocrystals distribute in the oxide matrix randomly in three dimensions, with the formation of more uncharged nanocrystals due to more electron release at a higher temperature, the electron tunneling via the uncharged nanocrystals will go beyond the two-dimension regime, making  $\zeta$  larger than  $5/3$ . Therefore, the current conduction of the system will evolve toward the three-dimension transport with temperature. For example,  $\zeta$  increases from 1.79 for  $Q_{ri}=0$  at  $25^\circ\text{C}$  to 2.10 for  $Q_{ri}=3.69 \times 10^{11} \text{ e/cm}^2$  at the temperature of  $200^\circ\text{C}$ , but it is always beyond the upper limit  $\zeta=5/3$  for two dimensional transport. This indicates that the current conduction of the system is a quasi-3D transport and evolves toward the 3D transport with more charge release. As can be observed from Fig. 4, the charge release leads to an increase in  $I_0$  also, which is due to the decrease of the tunneling resistance and/or the increase in the number of tunneling paths as a result of the charge release at a higher temperature.<sup>12</sup> Fittings to the data of  $I_0$  and  $\zeta$  shown in Fig. 4 yield the following phenomenological mathematical expres-

sions:  $I_0 = 4.12 \times 10^{-9} \exp(1.95 \times 10^{-11} Q_{ri})$  and  $\zeta = 7.7 \times 10^{-13} Q_{ri} + 1.82$ . As given by the expressions, for the initial state at room temperature, i.e.,  $Q_{ri}=0$ ,  $I_0$  is  $4.12 \times 10^{-9} \text{ AV}^{-\zeta}$ , which is actually the  $I_0$  at room temperature; and  $\zeta = 1.82$ , which is larger than  $5/3$ , suggesting that the current transport at room temperature is beyond the two-dimension regime and is a quasi-3D transport.

Note that charging and discharging can occur during electrical measurement and they are random processes. As such,  $I$ - $V$  measurement at a given temperature is not necessarily repeatable. For example, the  $I$ - $V$  characteristic after back from the measurement at  $100^\circ\text{C}$  to room temperature ( $25^\circ\text{C}$ ) can be different from the initial  $I$ - $V$  characteristic at room temperature. The current level of the former can be either higher or lower than that of the latter.

In conclusion, Al/Al<sub>2</sub>O<sub>3</sub> nanocomposite films are prepared with RF magnetron sputtering of Al target in O<sub>2</sub> ambient. MIS structures are formed by coating an Al layer on the top of the films. The  $I$ - $V$  characteristic of the system at low fields follows a power law, i.e.,  $I = I_0 (V - V_{th})^\zeta$  where the threshold voltage  $V_{th} \approx 0$  and the factors  $I_0$  and  $\zeta$  increase with the charge release from the nanocrystals when the temperature increases. The charge release from nanocrystals causes an increase of  $I_0$  because of the decrease in the resistance of the tunneling paths and/or the formation of more tunneling paths due to more neutral nanocrystals available. On the other hand,  $\zeta$  also increases, showing an evolution of the current conduction with a trend toward the 3D transport.

## ACKNOWLEDGMENTS

This work has been financially supported by NSFC under project No. 60806040, the Fundamental Research Funds for the Central Universities under project No. ZYGX2009X006, the Young Scholar Fund of Sichuan under project No. 2011JQ0002 and the National Research Foundation of Singapore under project NRF-G-CRP 2007-01.

- <sup>1</sup>Z. Jin, H. S. Kwok, and M. Wong, *IEEE Electron Device Lett.* **19**, 502 (1998).
- <sup>2</sup>O. Auciello, W. Fan, B. Kabius, S. Saha, J. A. Carlisle, R. P. H. Chang, C. Lopez, E. A. Irene, and R. A. Baragiola, *Appl. Phys. Lett.* **86**, 042904 (2005).
- <sup>3</sup>J.-C. Chiang and J.-G. Hwua, *Appl. Phys. Lett.* **90**, 102902 (2007).
- <sup>4</sup>S. Choi, S. S. Kim, H. Yang, M. Chang, S. Jeon, C. Kim, D. Y. Kim, and H. Hwang, *Microelectron. Eng.* **80**, 264 (2005).
- <sup>5</sup>S. K. Kim, Y. Xuan, P. D. Ye, S. Mohammadia, J. H. Back, and M. Shim, *Appl. Phys. Lett.* **90**, 163108 (2007).
- <sup>6</sup>J. B. Koo, C. H. Ku, S. C. Lim, S. H. Kim, and J. H. Lee, *Appl. Phys. Lett.* **90**, 133503 (2007).
- <sup>7</sup>W. Zhu, T. P. Chen, Z. Liu, M. Yang, Y. Liu, and S. Fung, *J. Appl. Phys.* **106**, 093706 (2009).
- <sup>8</sup>S. Nakata, K. Saito, and M. Shimada, *Appl. Phys. Lett.* **87**, 223110 (2005).
- <sup>9</sup>J. I. Wong, T. P. Chen, M. Yang, Y. Liu, C. Y. Ng, and L. Ding, *J. Appl. Phys.* **106**, 013718 (2009).
- <sup>10</sup>M. Yang, T. P. Chen, Z. Liu, J. I. Wong, W. L. Zhang, S. Zhang, and Y. Liu, *J. Appl. Phys.* **106**, 103701 (2009).
- <sup>11</sup>R. Krishnan, Q. Xie, J. Kulik, X. D. Wang, S. Lu, M. Molinari, Y. Gao, T. D. Krauss, and P. M. Fauchet, *J. Appl. Phys.* **96**, 654 (2004).
- <sup>12</sup>C. Y. Ng, Y. Liu, T. P. Chen, and M. S. Tse, *Smart Mater. Struct.* **15**, S43 (2006).
- <sup>13</sup>Y. Liu, T. P. Chen, C. Y. Ng, M. S. Tse, S. Fung, Y. C. Liu, S. Li, and P. Zhao, *Electrochem. Solid-State Lett.* **7**, G134 (2004).
- <sup>14</sup>Y. Liu, T. P. Chen, P. Zhao, S. Zhang, S. Fung, and Y. Q. Fu, *Appl. Phys. Lett.* **87**, 033112 (2005).
- <sup>15</sup>A. A. Middleton and N. S. Wingreen, *Phys. Rev. Lett.* **71**, 3198 (1993).
- <sup>16</sup>H. E. Romero and M. Drndic, *Phys. Rev. Lett.* **95**, 156801 (2005).